

Coulomb screening in linear coasting nucleosynthesis

Parminder Singh*¹ and Daksh Lohiya^{†2}

¹Dronacharya Government College, Gurugram University, Gurugram, INDIA

²Department of Physics and Astrophysics, University of Delhi,, Delhi 110007, INDIA.

August 16, 2023

Abstract

We investigate the impact of coulomb screening on primordial nucleosynthesis in a universe having scale factor that evolves linearly with time. Coulomb screening affects primordial nucleosynthesis via enhancement of thermonuclear reaction rates. This enhancement is determined by the solving Poisson equation within the context of mean field theory (under appropriate conditions during the primordial nucleosynthesis). Using these results, we claim that the mean field estimates of coulomb screening hardly affect the predicted element abundances and nucleosynthesis parameters, $\{\eta_9, \xi_e\}$. The deviations from mean field estimates are also studied in detail by boosting genuine screening results with the screening parameter (ω_s). These deviations show negligible effect on the element abundances and on nucleosynthesis parameters. This work thus rules out the coulomb screening effects on primordial nucleosynthesis in slow evolving models and confirms that constraints in ref. [7] on nucleosynthesis parameters remain unaltered.

1 Introduction

“Power Law Cosmologies” in which the scale factor evolves as $a(t) \sim t^n$ with $n \geq 1$ have emerged as a potential alternative to the standard cosmological models. It is being free of issues found in the standard scenario like the flatness problem, horizon problem, identification of dark matter components etc. [1, 2]. The power law models can be motivated either in the framework of conformal gravity [2] or by considering non-minimally coupled unstable scalar fields in the FRW scenario [3]. Particularly interesting model in this class of cosmologies is the linearly coasting universe with $n = 1$. Even though quite simple, this special case has been found to be concordant with the many observational features such as the SNe1a data [4, 5], lensing statistics [6] and the primordial nucleosynthesis [7, 8, 9].

It was shown in ref.[7] that primordial nucleosynthesis in a Linearly Coasting Cosmology (LCC) can *successfully* achieve the observed levels of ^4He [10] and the minimum metallicity levels ($Z_{cr} \sim 10^{-6} Z_\odot$) within the allowed ranges of baryonic density (Ω_B) and puts a constraint on the electron neutrino degeneracy parameter (ξ_e). Such constraints on Ω_B saturates the matter content of universe by baryons alone and eliminates “Dark Matter Problem”. The order of primordial metallicity achieved in the process also removes the need of hypothetical PopIII stars of standard cosmological models which are required for the

*parminderofficial.du@gmail.com

[†]dl116@cam.ac.uk

fragmentation, cooling and formation process of proto-stellar clouds as they form observed lowest metal stars [11, 12, 13, 14].

It has been argued in ref. [15] that coulomb screening during the primordial nucleosynthesis may have an effect on the nuclear reaction rates and can enhance the nucleosynthesis process which could change the estimates of the parameters Ω_B in LCC. Such a screening mechanism can be studied as follows. At the epoch of nucleosynthesis, the temperature of the universe is of the order of MeVs and the universe consists of a hot plasma containing photons, electron-positron pairs, neutrinos and antineutrinos of three flavours and a very small amount of baryons [7]. In this plasma, charged particle number density is dominated by the e^\pm pairs [15]. Any two nuclides having charges Z_1e and Z_2e will be screened by the negatively charged electrons of the plasma. This screening of nuclei charges by the electron cloud reduces the coulomb potential of these charges and would enhance the rate of nuclei interaction. This has been studied in great detail for stellar interiors in refs. [16, 17, 18, 19, 20, 21, 22]. One can also calculate the coulomb screening for the early universe by using the well-known mean field approximation but with appropriate modifications. This can then be incorporated in the nuclear reaction rates. This is a completely different task than the standard BBN where the reaction network contains only 88 reactions and 26 nuclide [23, 24, 25, 26, 27, 28] because only light elements can be synthesized up to the observed levels due to rapid expansion of universe and a very little amount of metallicity is produced ($Z \sim \mathcal{O}(10^{-16})$) [29]. The modified nucleosynthesis code for the linear evolution of the scale factor [30] on the other hand considers a heavy network of 557 reaction rates and 130 nuclide since heavy elements (eg. CNO) can easily be produced upto appreciable levels in this framework. This has its roots in the slower expansion rates of the universe [7]. In order to determine the correct amount of nuclide abundance, this nucleosynthesis network requires details of nuclear reaction rates $\langle\sigma v\rangle$, which depend upon cross-section ' σ ' and relative velocity ' v ' of interacting nuclides governed by the Maxwell-Boltzmann distribution for a particular temperature ' T '. The detailed calculations of $\langle\sigma v\rangle$ are discussed in [31, 32, 33]. Any correction in the nuclear reaction rates on account of coulomb screening can change the nuclides abundances which directly affects the constraints on nucleosynthesis parameters.

With this motivation, we first review the screening in the early universe using mean field theory and solve the relevant Poisson equation numerically in Section 2. This would give the reaction rate enhancement factor of two nuclei with charge Z_1e and Z_2e during nucleosynthesis. In Section 3, we determine the important reaction rates which play key role during the peak activity of nucleosynthesis process in the formation and destruction of a particular nuclide. In Section 4, we further elaborate how coulomb screening affects nucleosynthesis parameters via nuclide abundances. This is qualitatively understood by restricting to the important reaction rates determined through processing rates. Finally, we also study the impact on nuclide abundances and nucleosynthesis parameters under any deviation from mean field approach.

2 Coulomb screening in the early universe

This section provides a brief review of coulomb screening which is required to determine the enhancement of the reaction rates between two interacting nuclei having charges Z_1e and Z_2e in the early universe. To determine the enhancement factor, we solve the Poisson equation numerically within the context of mean field theory on the similar lines as described in ref. [16] for the stellar cases. During nucleosynthesis, when the temperature of the universe is of the order of few MeVs, the charged particle number density is dominated by the e^\pm pairs.

This number density of electron-positron is given by the Fermi-Dirac distribution having momenta in the

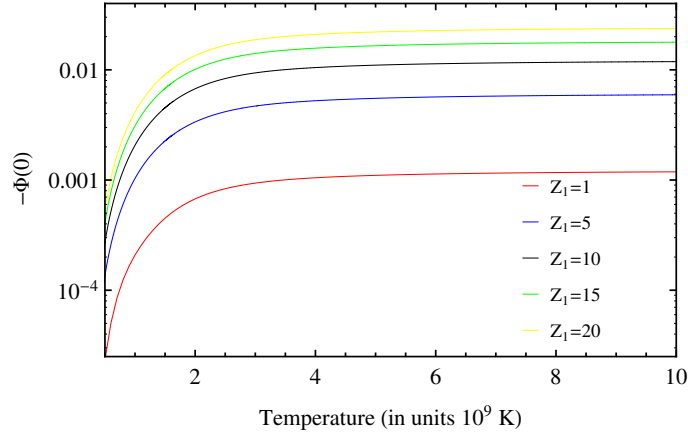


Figure 1: Plot of $-\Phi(0)$ as a function of Temperature (in units 10^9 K) for different nuclei charges (Z_1).

range p to $p + dp$ at any temperature, T with a chemical potential μ , as [34]:

$$n_{e\pm}(p) = \frac{8\pi}{h^3} \int_0^\infty p^2 dp \left[1 + \exp\left(\frac{E(p) \pm \mu}{kT}\right) \right]^{-1} \quad (1)$$

where $E(p) = p^2 c^2 + m_e^2 c^4$ represents the energy of particles.

We replace variables, $p/m_e c = \eta$, $m_e c^2/kT = z$ and rearrange Eq. (1) as

$$n_{e\pm}(\mu, T) = \kappa I_{\pm}(\mu, T) \quad (2)$$

Here, $\kappa = \pi^{-2} (m_e c/\hbar)^3$ and

$$I_{\pm}(\mu, T) = \int_0^\infty \frac{\eta^2 d\eta}{1 + \exp(z(\eta^2 + 1)^{1/2} \pm \mu/kT)}$$

In this electron-positron plasma, we consider a nucleus having charge $Z_1 e$ at the origin. We can then write the total electrostatic potential, $U_{tot}(r)$ at any point 'r' from this origin. This potential can be given by the sum of coulomb potential of the bare nucleus and some unknown potential $V(r)$:

$$U_{tot}(r) = Z_1 e/r + V(r) \quad (3)$$

Here $V(r)$ is the mean potential which is given by all the charged particles of plasma except the nucleus Z_1 . This is also termed as the screening potential because it screens the coulomb potential experienced by any interacting charged nuclei at that point. This reduction in coulomb potential through $V(r)$ would enhance the rate of interaction between Z_1 and some another interacting nucleus Z_2 . In ref. [16], Salpeter demonstrated that enhancement factor E_s in the rate of interaction between the nuclei Z_1 and Z_2 will only require $V(0)$, i.e. the screening potential at the origin instead of $V(r)$.

This enhancement factor is given by:

$$E_s = \exp\left(\frac{-Z_2 e V(0)}{kT}\right). \quad (4)$$

Eq. (4) reduces our problem to solve screening potential at origin only.

For the calculation of $V(0)$, we need to solve the Poisson equation which is given by

$$\nabla^2 U_{tot}(r) = -4\pi en(r) - 4\pi Z_1 e\delta^3(r) \quad (5)$$

This, then, reduces to the following form for the potential $V(r)$:

$$\nabla^2 V(r) = -4\pi en(r). \quad (6)$$

Here, $n(r)$ represents the effective number density at distance ‘ r ’ from the nucleus Z_1 due to the electrons and the positrons which is given by

$$n(r) = n_{e^+}(\mu, T, U_{tot}(r)) - n_{e^-}(\mu, T, U_{tot}(r)) \quad (7)$$

in terms of the modified Fermi-Dirac distribution. This modification occurs since the electrons and the positrons at ‘ r ’ experience an interaction energy equal to $eU_{tot}(r)$. Then their number densities will no longer be left uniform and will arrange themselves in such a way that the total thermodynamic potential is uniform. This modified distribution is given by:

$$n_{e^\pm}(\mu, T, U_{tot}(r)) = \kappa I_\pm(\mu, T, U_{tot}(r))$$

with

$$I_\pm(\mu, T, U_{tot}) = \int_0^\infty \frac{\eta^2 d\eta}{1 + \exp(z(\eta^2 + 1)^{1/2} \pm (\mu/kT + eU_{tot}/kT))} \quad (8)$$

In the early universe, the chemical potential corresponding to the electrons and positrons is negligibly small, $\mu \approx 0$ [27, 34] and hence we can write,

$$n_{e^\pm}(0, T, U_{tot}(r)) = \kappa I_\pm(0, T, U_{tot}(r)). \quad (9)$$

We also need to impose the boundary conditions in order to solve for the potential. For this, we can take that at large distances,

$$U_{tot}(r) \rightarrow 0 \quad \text{as } r \rightarrow \infty. \quad (10)$$

This makes sure that at sufficiently large distances, the number density of electrons and positrons returns to its field free value

$$n_\infty = n_{e^-}(0, T, 0) = n_{e^+}(0, T, 0) = \kappa I(T). \quad (11)$$

with

$$I(T) = \int_0^\infty \frac{\eta^2 d\eta}{1 + \exp(z(\eta^2 + 1)^{1/2})} \quad (12)$$

Using Eqs. (7) and (11) in Eq. (6), we have

$$\nabla^2 V(r) = 4\pi en_\infty \left(\frac{I_-(0, T, U_{tot}(r)) - I_+(0, T, U_{tot}(r))}{I(T)} \right) \quad (13)$$

Defining new variables,

$$\begin{aligned} \Phi(r) &\equiv \frac{eV(r)}{kT}, & R &\equiv \left(\frac{kT}{4\pi e^2 n_\infty} \right)^{1/2}, \\ x &\equiv \frac{r}{R}, & F &\equiv \frac{Z_1 e^2}{RkT}, \end{aligned} \quad (14)$$

Table 1: Shows the numerical value of $\Phi_1(0)$ with Temperature (in units 10^9 K).

Temperature (in units $10^9 K$)	$-\Phi_1(0)$ ($-\Phi(0)$ for $Z_1=1$)
100.0	1.24×10^{-3}
50.0	1.24×10^{-3}
20.0	1.21×10^{-3}
10.0	1.19×10^{-3}
5.0	1.10×10^{-3}
2.0	6.74×10^{-4}
1.0	2.09×10^{-4}
0.5	2.33×10^{-5}
0.3	7.71×10^{-7}
0.1	4.51×10^{-15}

where, R is defined as screening radius and F is the screening strength parameter which is defined by the ratio of coulomb interaction at screening radius and the average kinetic energy of the particle. This parameter also governs the weak ($F \ll 1$), intermediate ($F \approx 1$) and the strong screening ($F \gg 1$) regimes. Using Eq. (14) in Eq. (13), we have

$$\nabla_x^2 \Phi(x) = \frac{1}{I(T)} \left(\int_0^\infty \frac{\eta^2 d\eta}{1 + \exp(z(\eta^2 + 1)^{1/2} - F/x - \Phi(x))} - \int_0^\infty \frac{\eta^2 d\eta}{1 + \exp(z(\eta^2 + 1)^{1/2} + F/x + \Phi(x))} \right) \quad (15)$$

Boundary conditions to solve Eq. (15) are such that $\Phi(x)$ approaches a finite value at the origin and approaches $-F/x$ as x tends to infinity. To solve Eq. (15) numerically it is found convenient to transform this equation to one involving $Z(x) = x\Phi(x)$. Then resultant equation after this transformation becomes

$$\frac{d^2 Z}{dx^2} = \frac{x}{I(T)} \left(\int_0^\infty \frac{\eta^2 d\eta}{1 + \exp(z(\eta^2 + 1)^{1/2} - (F + Z(x))/x)} - \int_0^\infty \frac{\eta^2 d\eta}{1 + \exp(z(\eta^2 + 1)^{1/2} + (F + Z(x))/x)} \right) \quad (16)$$

with the boundary conditions $Z(0) = 0$ and Z approaching $-F$ as x tends to infinity. We solve this equation numerically on the lines of ref. [16] with these boundary conditions to determine the value of $\Phi(0)$. We plot value of $-\Phi(0)$ as a function of temperature for different values of Z_1 in Fig. 1. This leads to an enhancement factor of reaction rates in the early universe

$$E_s = \exp(-Z_2 \Phi(0)) \quad (17)$$

Our numerical results are in good agreement with the results of Itoh et al [27] and approximated by:

$$E_s = \exp(-Z_1 Z_2 \Phi_1(0)) \quad (18)$$

where, $\Phi_1(0)$ is defined as $\Phi(0)$ for $Z_1 = 1$. Numerical values of $\Phi_1(0)$ as function of temperature are shown in Table 1.

3 Processing Rates

To determine the primordial element abundances, the numerical calculation requires a network of nuclear reaction rates. In LCN, this network determines 130 element abundances via 557 reactions which is quite large in comparison with SBBN which has only 88 reactions. But all these reactions are not equally important and only a few of them dominate during nucleosynthesis. These key reaction rates are important for the qualitative understanding of screening effects during nucleosynthesis process and also help in the quantitative study of nucleosynthesis in such slow evolving models. So it is important to discuss the method to determine the key reactions in the Linear coasting nucleosynthesis.

To know the key reaction rates, we have to calculate the processing rate for individual reaction as a function of temperature and list them according to their importance during peak activity of nucleosynthesis. To figure out the processing rates, we consider a reaction in which nuclei ‘ a ’ is produced through ‘ c ’ and ‘ d ’ and destroyed on the interaction with nuclei ‘ b ’. This reaction can be written as:



We define the processing rate ‘ $P_{\text{prod}}(d(c, b)a)$ ’ for the production of ‘ a ’ via c and d as

$$P_{\text{prod}}(d(c, b)a) \equiv \frac{\rho_b N_A \langle \sigma v \rangle_{cd} Y_c Y_d}{H} \quad (20)$$

where, $Y_i \equiv X_i/A_i$, X_i is the mass fraction contained in the nuclei with atomic mass A_i , ρ_b is the baryonic density of the universe and $\langle \sigma v \rangle_{cd}$ represent the rate of this interaction.

Similarly, we can write the processing rate for the destruction of ‘ a ’ nuclide on interacting with ‘ b ’ nuclide as

$$P_{\text{dest}}(a(b, c)d) \equiv \frac{\rho_b N_A \langle \sigma v \rangle_{ab} Y_a Y_b}{H} \quad (21)$$

where, H is hubble expansion rate.

In Standard Big Bang Nucleosynthesis(SBBN), only 12 reactions play a significant role for the formation of lighter nuclei [35]. For the linear coasting nucleosynthesis, ${}^4\text{He}$ and metallicity (Z) is produced upto observed level. The following reactions significantly affect the production of ${}^4\text{He}$ in LCN:

- $\text{D(p,g)}{}^3\text{He}$, ${}^3\text{He(d,p)}{}^4\text{He}$
- $\text{T(p,n)}{}^3\text{He}$, $\text{T(p,g)}{}^4\text{He}$

and ${}^4\text{He}$ mainly destructs through the following reactions:

- $\text{D(a,g)}{}^6\text{Li}$
- $\text{T(a,g)}{}^7\text{Li}$
- ${}^3\text{He(a,g)}{}^7\text{Be}$, ${}^3\text{He(a,p)}{}^6\text{Li}$

Metallicity (Z) gets significantly produced by the following set of reactions:

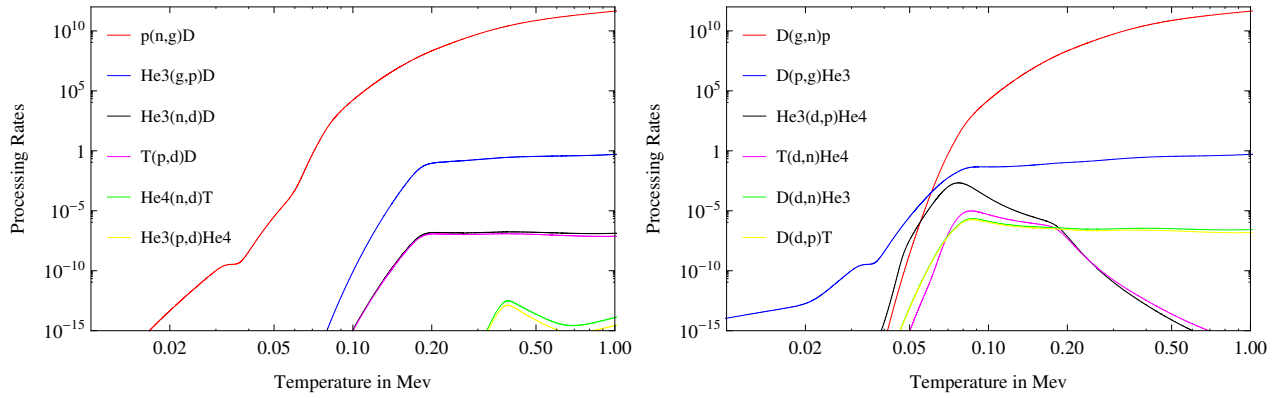


Figure 2: Left Panel: Show the processing rates for Deuterium(D) production channels.
 Right Panel: Show the processing rates for Deuterium(D) destruction channels.

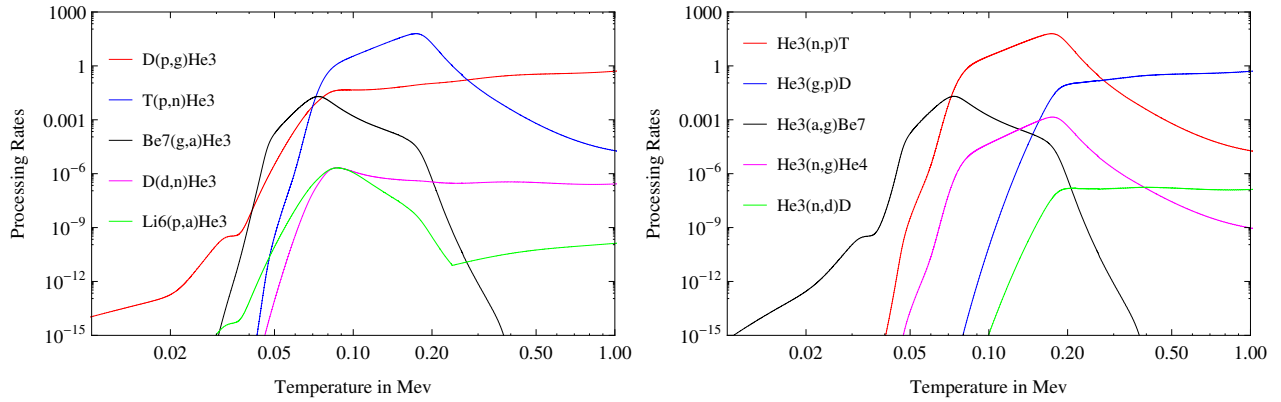


Figure 3: Left Panel: Show the processing rates for Helium-3(^3He) production channels.
 Right Panel: Show the processing rates for Helium-3(^3He) destruction channels.

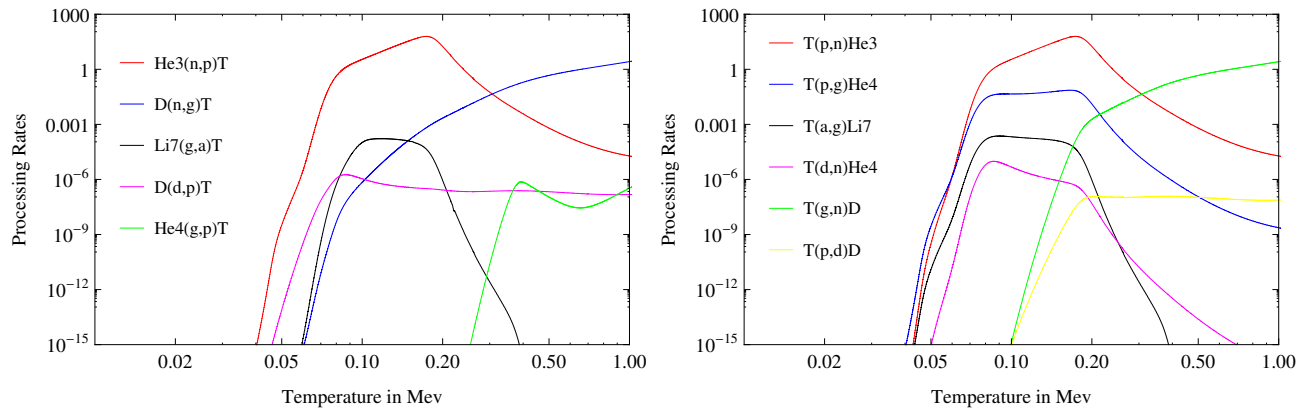


Figure 4: Left Panel: Show the processing rates for Tritium(T) production channels.
 Right Panel: Show the processing rates for Tritium(T) destruction channels.

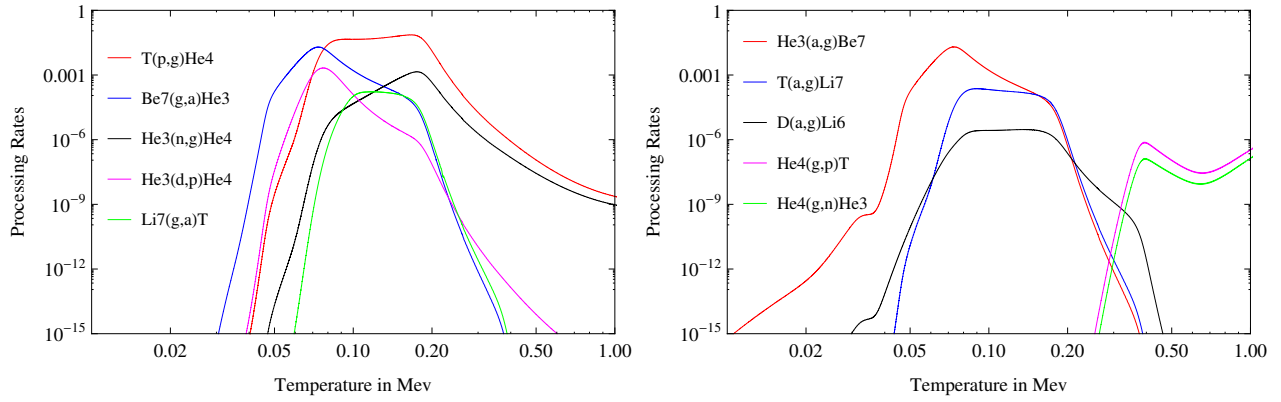


Figure 5: Left Panel: Show the processing rates for Helium-4 (${}^4\text{He}$) production channels.
 Right Panel: Show the processing rates for Helium-4 (${}^4\text{He}$) destruction channels.

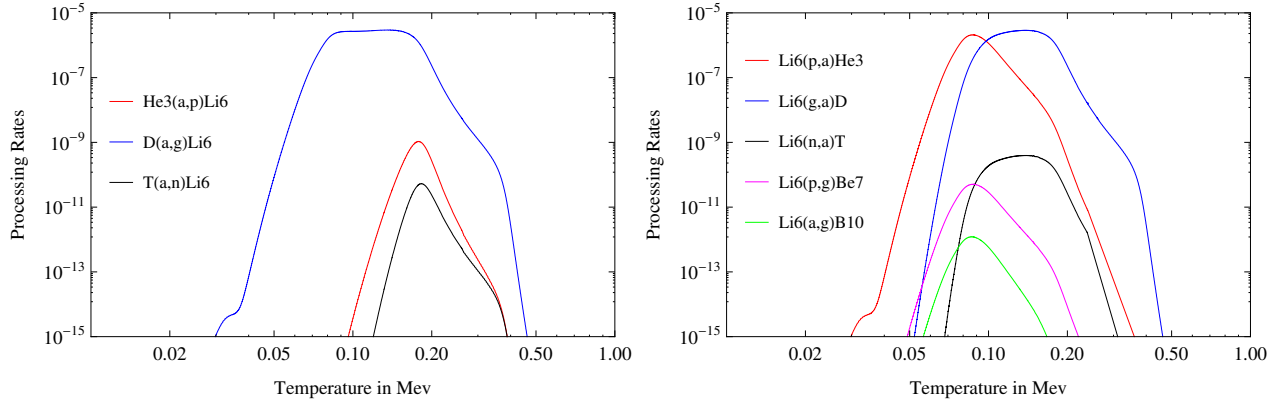


Figure 6: Left Panel: Show the processing rates Lithium-6 (${}^6\text{Li}$) production channels.
 Right Panel: Show the processing rates for Lithium-6 (${}^6\text{Li}$) destruction channels.

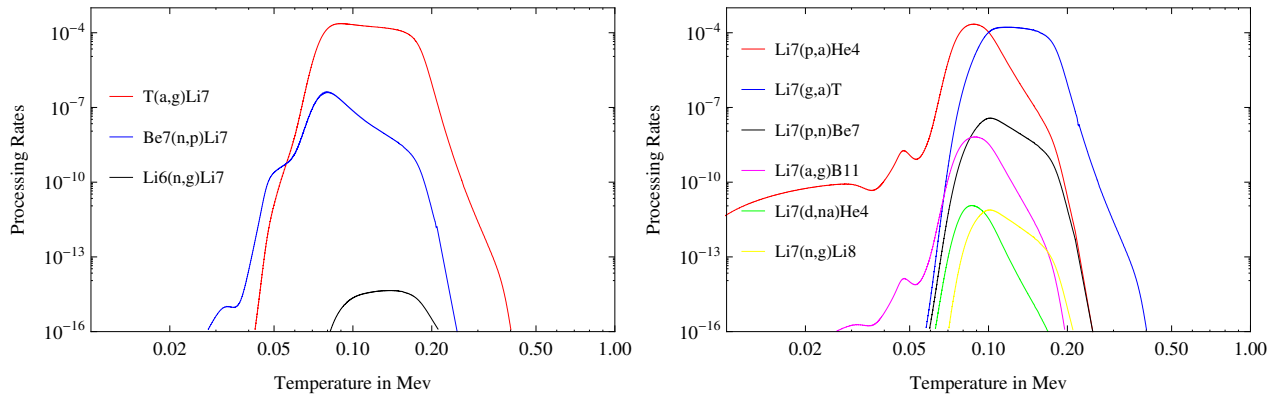


Figure 7: Left Panel: Show the processing rates Lithium-7 (${}^7\text{Li}$) production channels.
 Right Panel: Show the processing rates for Lithium-7 (${}^7\text{Li}$) destruction channels.

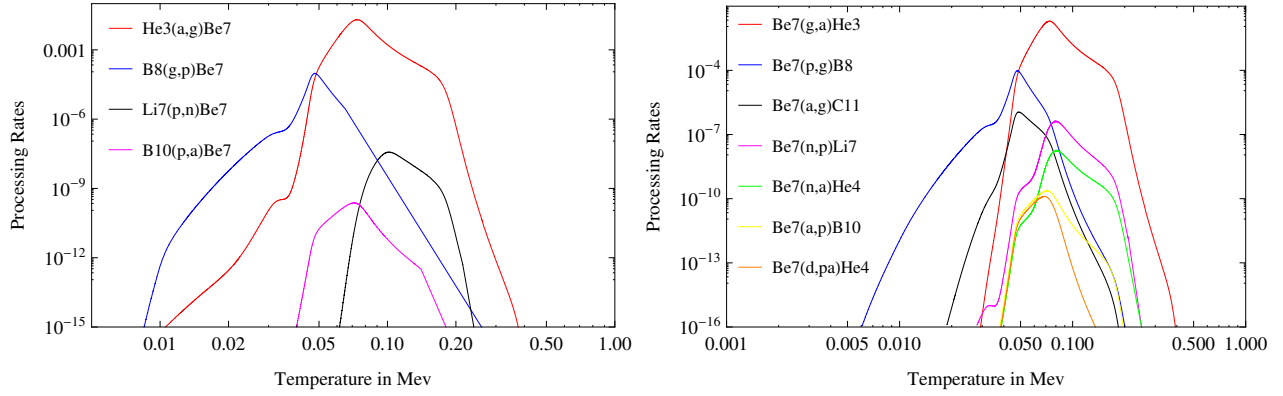


Figure 8: Left Panel: Show the processing rates for Be-7(${}^7\text{Be}$) production channels. Right Panel: Show the processing rates for Be-7(${}^7\text{Be}$) destruction channels.

- ${}^7\text{Be}(p,g){}^8\text{B}$, ${}^7\text{Be}(a,g){}^{11}\text{C}$, ${}^7\text{Be}(a,p){}^{10}\text{B}$
- ${}^7\text{Li}(p,n){}^7\text{Be}$, ${}^7\text{Li}(a,g){}^{11}\text{B}$
- ${}^6\text{Li}(p,g){}^7\text{Be}$, ${}^6\text{Li}(a,g){}^{10}\text{B}$

as shown by Figs. 2 - 8 where we have plotted the processing rates for the key elements as function of temperature in MeVs . One of the important feature of these plots is that the qualitative behaviour remains unchanged for different values of baryon to photon ratio(η_B) and electron neutrino degeneracy parameter(ξ_e).

4 Coulomb Screening and Nucleosynthesis Parameters

Our previous work showed that the primordial element abundances are very sensitive to two important nucleosynthesis parameters viz.; the baryon to photon ratio (η_B) and the electron neutrino degeneracy parameter (ξ_e) [7]. The baryon to photon ratio (η_B) can also be written as:

$$\eta_9 = 10^9 \eta_B \quad ; \quad \eta_9 = 27.39 \Omega_B h^2 \quad (22)$$

These nucleosynthesis parameters are tightly constrained within the context of LCN (without screening) in ref.[7] to be

$$\begin{aligned} \eta_9 &= 3.927 \pm 0.292 \quad ; \quad \Omega_B = 0.263 \pm 0.026 \\ \xi_e &= -2.165 \pm 0.171. \end{aligned} \quad (23)$$

These parameters are estimated such that they produce the observationally inferred ${}^4\text{He}$ abundance [10]

$$Y_p = 0.254 \pm 0.003 \quad (24)$$

and meet the minimum metallicity level (Z) required for the cooling and fragmentation process of the observed low metal stars in the universe given as:

$$Z = Z_{cr} = 10^{-6} Z_{\odot}. \quad (25)$$

Here, Z_{\odot} represents solar metallicity and the bounds for solar metallicity are given as [36]:

$$0.0187 \leq Z_{\odot} \leq 0.0239. \quad (26)$$

With these constraints on parameters, one can also produce an appreciable amount of CNO in comparison with SBBN [7]. These levels of CNO essentially required to sustain CNO cycle in the massive stars [37]. We now incorporate the screening effects discussed in Section 2 enhancing all the nuclear reactions rates considered in the network of 557 reactions except the weak interactions, neutron and gamma induced reactions. However, it is found that this screening is unable to produce any measurable impact on primordial abundances of ${}^4\text{He}$ and Z as well as on nucleosynthesis parameter. This can qualitatively be apprehended by using the processing rates from which we get the reaction rates that dominantly affect ${}^4\text{He}$ and Z abundances as discussed in Section 3.

Most of the reactions in ${}^4\text{He}$ production channel have $Z_1 \times Z_2=1$ with a maximum enhancement of:

$$\exp(1.24 \times 10^{-3}) \sim 1.00124 \quad (27)$$

at high temperatures and it decreases sharply as the temperature decreases. Similarly the metallicity production reaction rates are only enhanced by:

$$\exp(6 \times 1.24 \times 10^{-3}) \sim 1.0075 \quad (28)$$

when produced via interaction between Lithium and ${}^4\text{He}$ in which $Z_1 \times Z_2=6$ and production through Beryllium and ${}^4\text{He}$ leads to an enhancement of

$$\exp(8 \times 1.24 \times 10^{-3}) \sim 1.01 \quad (29)$$

where, $Z_1 \times Z_2 = 8$. In this way, the coulomb screening can enhance the reaction rates only upto one percent.

Such an enhancement hardly impacts the previous results obtained without incorporating the screening. Thus, we can safely use the constraints on nucleosynthesis parameters as given in Eq. (23).

However, it is interesting to see how any deviation from the mean field approximation can affect the element abundances and the nucleosynthesis parameters. To understand such deviations, we can artificially modify our screening result by rescaling the screening potential by some screening parameter ω_s which is defined in the following way:

$$E'_s = \exp(-\omega_s Z_2 Y(0)); \quad \omega_s = \ln E_s / \ln E'_s. \quad (30)$$

with ω_s that can be considered to be lying in a range between 0 and 100. We can then calculate percentage variation of any element abundance as function of ω_s which is given by:

$$\Delta(\omega_s) = \frac{Y_A(\omega_s) - Y_A(\omega_s = 0)}{Y_A(\omega_s = 0)}. \quad (31)$$

where $Y_A(\omega_s)$ and $Y_A(\omega_s = 0)$ represent any general element abundance for a screening parameter value ω_s and without any coulomb screening respectively. We plot this percentage variation as a function of screening parameter for the nuclides which are produced upto appreciable levels in such slowly evolving cosmologies as shown in Fig. 10. This plot clearly shows that ${}^4\text{He}$ is very less sensitive to the screening parameter in

comparison with metallicity (Z). Thus, as the screening parameter increases the dominant nuclear reaction rates involved in the production of metallicity are highly enhanced with respect to ${}^4\text{He}$ as demonstrated in Eqs. (27 - 29).

We also determine the flow of nucleosynthesis parameters as a function of screening parameter by

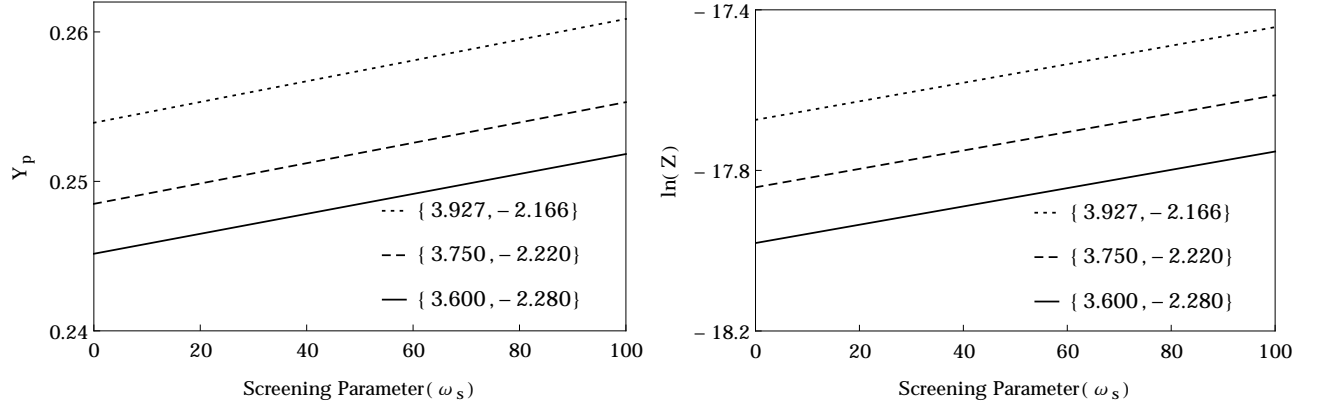


Figure 9: Left and Right Panel demonstrate the linear response of ${}^4\text{He}$ abundance(Y_p) and Metallicity ($\ln(Z)$) respectively with screening parameter(ω_s). For an individual linear plot we fix baryon to photon ratio, η_9 (in units 10^9) and electron degeneracy parameter, ξ_e and represented as $\{\eta_9, \xi_e\}$.

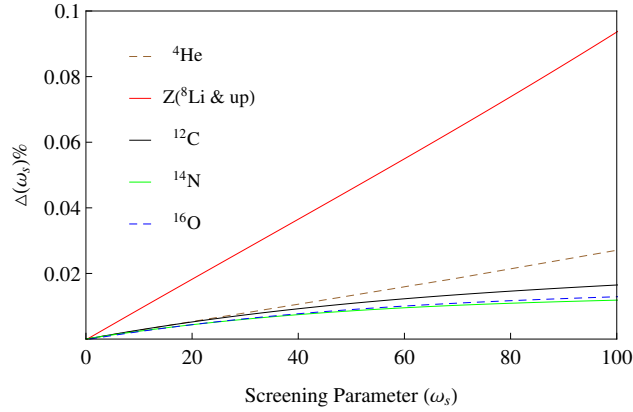


Figure 10: Percentage variation ($\Delta(\omega_s)\%$) of predicted elemental abundances with the screening parameter(ω_s).

defining a general fitting function for ${}^4\text{He}(Y_p)$ and Z in which the screening parameter (ω_s) is also included

$$Y_p = A_0 + B_0 \ln(\eta_9) + C_0 \xi_e + \omega_s (A + B \ln(\eta_9) + C \xi_e) \quad (32)$$

$$\ln(Z) = D_0 + E_0 \ln(\eta_9) + F_0 \xi_e + \omega_s (D + E \ln(\eta_9) + F \xi_e) \quad (33)$$

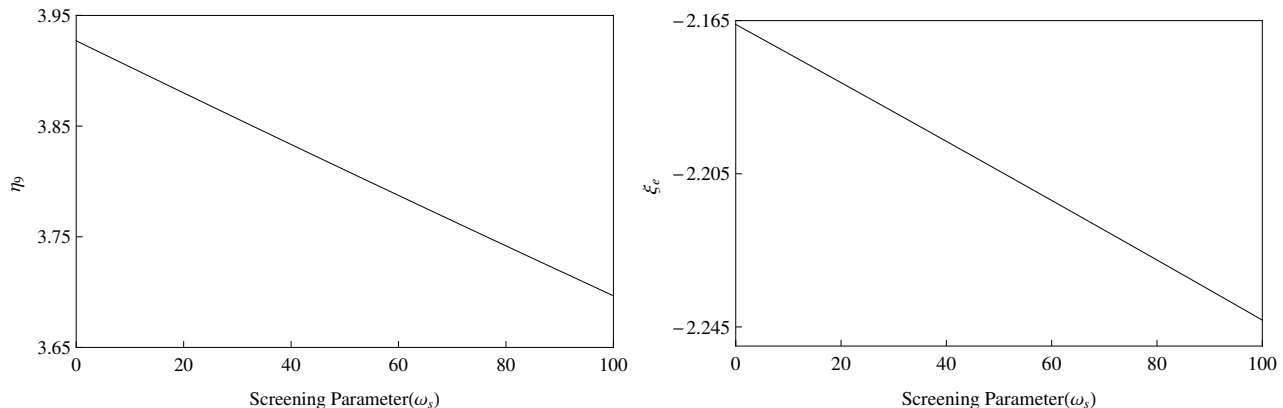


Figure 11: Left Panel: Variation of baryon to photon ratio, η_9 (in units 10^9) as a function of screening parameter(ω_s). Right Panel: Flow of electron neutrino degeneracy parameter(ξ_e) with screening parameter(ω_s).

The coefficients are found to be:

$$\begin{aligned}
 A_0 &= -0.5065; B_0 = 0.3102; C_0 = -0.1554 \\
 A &= 3.516 \times 10^{-6}; B = 3.983 \times 10^{-5}; C = -5.344 \times 10^{-6} \\
 D_0 &= -30.4804; E_0 = 6.2832; F_0 = -1.9555 \\
 D &= 1.902 \times 10^{-4}; E = 8.983 \times 10^{-4}; F = -4.119 \times 10^{-4}
 \end{aligned}$$

In this model, we use the fact that the Y_p and $\ln(Z)$ both are varying linearly with ω_s as shown in Fig. 9. Using constraints of Y_p and Z values from Eqs.24 and 25 in the above fitted equations we can solve for $\ln(\eta_9)$ and ξ_e to get

$$\ln(\eta_9) = \frac{1.368 - 7.232 \times 10^{-4}\omega_s - 3.138 \times 10^{-9}\omega_s^2}{1. - 8.783 \times 10^{-5}\omega_s - 3.138 \times 10^{-8}\omega_s^2} \quad (34)$$

$$\xi_e = - \left(\frac{2.165 + 6.414 \times 10^{-4}\omega_s + 3.143 \times 10^{-8}\omega_s^2}{1. - 5.344 \times 10^{-5}\omega_s - 3.44 \times 10^{-8}\omega_s^2} \right) \quad (35)$$

Note that, these solutions for the parameters are only valid for the range of ω_s lying between 0 to 100. We plot η_9 and ξ_e as a function of ω_s in Fig. 11. These plots abundantly show that the baryon to photon ratio (η_9) decreases and the electron neutrino degeneracy parameter(ξ_e) becomes more negative with ω_s respectively. This suggests that, even by enhancing the coulomb screening effects 100 times, the nucleosynthesis parameters lie with in the error bars of the previous work [7]. Hence, we conclude that the coulomb screening does not form any key ingredient for the primordial nucleosynthesis even in slow evolving cosmological models.

5 Discussion and Conclusion

In this article, we have considered the effect of coulomb screening on the primordial nucleosynthesis in a linearly coasting universe via nuclear reaction rates. It was suggested in ref. [15] that coulomb screening

during the primordial nucleosynthesis may have an effect on the nuclear reaction rates in Linearly coasting universe. To determine the screening effect, we used the mean field approximation and solved the Poisson equation in the appropriate conditions that exist during primordial nucleosynthesis in linearly coasting universe. Due to lack of analytical solutions, we integrate this equation numerically using appropriate boundary conditions. These numerical results are in good agreement with the results of Itoh et al.

In order to interpret the whole effect of coulomb screening qualitatively we also determined the key reaction rates from 557 reactions which significantly affect the element abundances. But it is important to note that the screening is incorporated in all the reactions (excludes weak interactions as well as gamma and neutron induced reactions). Incorporating screening effects in LCN leads to negligibly small impact on nuclide abundances as well as on nucleosynthesis parameter $\{\eta_9, \xi_e\}$.

We also show how any deviations from the mean field approximation can effect the nuclide abundances and parameters. This was studied by defining a screening parameter (ω_s) to boost the screening effects. The ${}^4\text{He}$ abundance shows a very slight dependence on ω_s in comparison with the metallicity (Z) levels. Even for large values of ω_s , the nucleosynthesis parameters cannot go beyond the error bounds of the previous work. This demonstrates that the coulomb screening does not play any key role in the primordial nucleosynthesis of slow evolving models. In any case such large deviations are not justifiable on any physical grounds. All the previous works suggest that this screening parameter is in good agreement with $\omega_s \sim 1$ and the claims in ref. [15] are not compatible even with large values of the screening parameter. This work strongly suggests that the observed amount of ${}^4\text{He}$ and minimum metallicity requirements (Z) can only be produced by a unique set of nucleosynthesis parameters in such a slow evolving cosmology.

References

- [1] P. D. Mannheim & J. G. O'Brien; *Phy. Rev. D*85, 124020, 2012.
- [2] P. D. Mannheim; *Phy. Rev. D*85, 124008, 2012.
- [3] L. H. Ford; *Phy. Rev. D*35, 2349, 1987.
- [4] A. Dev, M. Sethi & D. Lohiya; *Phy. Lett B* 504, 207-212, 2001.
- [5] G. Sethi, A. Dev & D. Jain; *Phy. Lett B* 624, 135-140, 2005.
- [6] A. Dev, M. Safanova, D. Jain & D. Lohiya; *Phy. Lett B* 548, 12-18, 2002.
- [7] P. Singh and D. Lohiya; *JCAP* 05(2015)061.
- [8] M. Sethi, A. Batra & D. Lohiya; *Phy. Rev. D*60, 108301, 1999.
- [9] A. Benoit-Levy, G. Chardin; *Astron. & Astrophys.*,537, A78, 2012.
- [10] Y. I. Izotov et al.; *Astron. & Astrophys.*, 558, A57, 2013.
- [11] R. Schneider, K. Omukai, A. K. Inoue & A. Ferrara; *MNRAS*, 369, 1437, 2006.
- [12] K. Omukai, T. Tsuribe, R. Schneider & A. Ferrara; *Astrophys.J.*, 626, 627, 2005.
- [13] E. Scannapieco, R. Schnieder & A. Ferrara; *Astrophys. J.* 589, 35-52, 2003.

- [14] J. M. Escude & M. J. Rees; arXiv:astro-ph/9701093.
- [15] P. Kumar & D. Lohiya; arXiv:astro-ph/0802.1124.
- [16] E. E. Salpeter; Au. J. Ph., 7, 373, 1954.
- [17] E. E. Salpeter & H. M. Van Horn; Astrophys. J.,155, 183, 1969.
- [18] N. Itoh et. al.; Astrophys. J., 218, 477, 1977.
- [19] N. Itoh et. al.; Astrophys. J., 234, 1079, 1979.
- [20] E. Schatzman; J. Phys. Rad. 9, 46, 1948;
- [21] E. Schatzman; Astrophys. J. 119, 464, 1954.
- [22] G. Keller; Astrophys. J., 118, 142, 1953.
- [23] R.V. Wagoner; Astrophys. J. Suppl. 18, 247, 1969.
- [24] R.V. Wagoner; Astrophys. J. 179, 343, 1973.
- [25] L. H. Kawano; Preprint FERMILAB-Pub-88/34-A, 1988.
- [26] L. H. Kawano; Preprint FERMILAB-Pub-92/04-A, 1992.
- [27] N. Itoh & A. Nishikawa; Astrophys. J.; 488, 507, 1997.
- [28] B. Wang, C. A. Bertulani & A. B. Balentekin; Phy. Rev. C83, 018801, 2011.
- [29] F. Iocco, G. Mangano, et. al.; Phy. Rev. D75, 087304, 2007.
- [30] See: <http://parmindercosmophysics.weebly.com/lcn-code.html>.
- [31] D. D. Clayton; Principles of Stellar Evolution and Nucleosynthesis, Mc-Graw Hill, New York, 1968.
- [32] W. A. Fowler et. al.; ARA&A, 5, 525, 1967, (FCZI).,
- [33] W. A. Fowler et. al.; ARA&A, 13, 69, 1975, (FCZII).,
- [34] S. Weinberg; Gravitation and Cosmology: Principles and Applications of the General Theory of Relativity(1972), John-Wiley and Sons.
- [35] M. S. Smith , L. H. Kawano & R. A. Malaney; Astrophys. J. Suppl., 85, 219S, 1993.
- [36] W. J. Chaplin, A. M. Serenelli, et al.; Astrophys.J., 179, 872-884, 2007.
- [37] P. Marigo, C. Chiosi, R. P. Kudritzki; Astron. & Astrophys., 399, 617-630, 2003.